Proceedings of the Korean Nuclear Society Autumn Meeting
Seoul, Korea, October 1999

Thermal Analysis of the Liquid Pb/Bi Spallation Target and the Proton Beam Window

Jae-Seon Cho, Chang-Hyun Chung
Seoul National University
Shinlim-dong 56-1, Kwanak-gu, Seoul, 151-742, Korea

Tae Y. Song, Won S. Park
Korea Atomic Energy Research Institute
P.O. Box 105 Yusung Taejon, 305-600, Korea

ABSTRACT

Computational analyses are performed to investigate the heat transfer and the temperature distribution characteristics of the target system used in the accelerator-driven subcritical reactor. Pb/Bi eutectic material is adopted as the target material and the cylindrical geometry is employed for this study. The proton beam is set to be 1GeV and 20mA with the circular shape (diameter=10cm). LAHET code is used to evaluate the heat generation rates in the target material. Also, computational fluid dynamics code FLUENT is used to analyze the two dimensional steady state temperature distribution and flow distribution in the liquid Pb/Bi target system. It is assumed that the target system has a vertical upstream of the liquid Pb/Bi and the proton beam is injected from the top of the liquid Pb/Bi target. Since the beam is injected to the liquid Pb/Bi target region, the local temperature rises to the high temperature very rapidly and the high temperature region is restricted to the local region. Also, we performed the thermal hydraulic analysis for the double window system.

I. INTRODUCTION

An important issue to be considered for nuclear fuel cycle is the treatment/disposal of long-lived high level radioactive nuclides in the spent fuel. This high-level radioactive waste can be reduced by transmutation. The technology development for nuclear wastes transmutation has been recently initiated in several developed countries. The concept of the accelerator-driven subcritical reactor (ADSR) is considered as the most appropriate method among many concepts related to transmutation [1]. The HYPER (Hybrid Power Extraction Reactor) is a high power, accelerator-based transmutation system which is being designed by KAERI (Korea Atomic Energy Research Institute) [2]. The ADSR concept offers the possibility to minimize plutonium, higher actinides, and environmentally hazardous fission products from the waste stream destined for permanent storage.

Because the ADSR is operated under the subcritical state, the target system providing source neutrons inside the reactor is needed in this reactor. A spallation neutron source is proposed using a high-energy (GeV order) proton beam with a high current of 20mA. The high-intensity neutron flux in the accelerator-driven system is caused by an interaction of incident protons with target nuclei which has an cascade character at incident energies around 1GeV [3]. Spallation target is one of the basic elements of an accelerator-driven system. Problems relating to the heat removal from the target and radiation damage stability of the target material can be well solved by using liquid metal target [4]. Some key issues for the

target are flow distributions, window cooling and the local hot spots inside the target region, and they are related to the thermal-hydraulic performance. Since the beam is irradiated into the target in the subcritical reactor, the effectiveness of the heat removal from the target is one of the important things to be considered carefully. The liquid target has an advantage in cooling, but has the defect of the beam window problem.

In this study, we selected Pb/Bi as a sample of the liquid material. Then we studied the basic thermal hydraulic characteristics of the target material by using simulation code. The beam is set to be 1GeV and 20mA with the circular shape (diameter=10cm). It is assumed that the proton beam is injected from the top. We performed the calculations for the two cases of a uniform intensity proton beam and a parabolic intensity proton beam. In this study, the temperature distribution and the velocity vector profile are investigated in the liquid Pb/Bi target system. Also, the beam window cooling is studied for the single and double window systems. Figure 1 shows the schematic diagram of the single and double window systesm.

II. CALCULATION GEOMETRY AND ASSUMPTION

The cylindrical forced convection target system is set to be 50cm in diameter and 100cm in height. Calculation analyses are performed in two-dimensional axi-symmetry cylindrical geometry. It is assumed that the Pb/Bi material enters into the target region from the bottom and passes through to the top of the target container. Three cases are selected according to the calculation geometry. Each case is shown in Figure 2. In the first case, it is assumed that the center of beam window with the diameter of 30cm is located 25cm away from the top of the liquid Pb/Bi target container. The calculation region is limited to the liquid Pb/Bi pool. In the second case, the middle region of the target container is narrowed to enhance the flow velocity and other conditions are same as those of the first case. The third case is that the steel window region is included in the calculation domain. The steel window is 2mm thick and the other geometry conditions are same as those of the second case.

We used LAHET code for the simulation of heat generation. More than 50% of the beam energy is deposited as heat in the target [5]. In Figure 2, the black region of the target represents the heat generation region by the proton beam injection. Table 1 shows the heat generation rates for each position of liquid Pb/Bi target in a uniform intensity proton beam calculation. The results show statistical fluctuations. Table 2 shows the heat generation rates for each position of liquid Pb/Bi target in a parabolic intensity proton beam calculation.

The general CFD code FLUENT was used to simulate the two-dimensional steady state thermal and flow distribution of the liquid target. The proton beam is injected vertically from the top. Initial fluid temperature of the entering Pb/Bi temperature is set at 613K. The calculation parameter is the liquid Pb/Bi inlet velocity which is varied form 1.1m/sec to 2.0m/sec. In this calculation, the central axis is set to be symmetric and the surfaces are set to be adiabatic boundaries. It is assumed that the heat generation rates is constant during the calculation.

In calculation of this study, we used an orthogonal coordinate transformation. This transformation is performed using the grid generation components of the FLUENT code.

III. ANALYSIS RESULTS

III-1. Uniform Intensity Proton Beam

The bottom inlet velocity of the liquid Pb/Bi is chosen as 1.1m/sec, 1.35m/sec, 1.5m/sec and 2.0m/sec. In the first case, the maximum temperature of the target is 1287K for the inlet velocity of 1.1m/sec and 984K for the inlet velocity of 2.0m/sec. The maximum temperature region is located just below the center of beam window. The reason for this is that the Pb/Bi

flow is not brisk because of the wall surface effect in the maximum temperature region. The velocity distribution result shows that the flow of the liquid Pb/Bi stagnates in this region. The velocity increases by about 50% at the outlet region than the inlet region because the outlet area decreases by about 30% than the inlet area. Figure 3 shows the temperature distribution and the velocity vector profile in the target for the inlet velocity of 1.1m/sec case. As shown in Figure 3, the maximum temperature is 1287K and the maximum velocity is 1.77m/sec. The temperature varies rapidly in the beam entrance region, and is almost uniform in the other region.

In the second case, the maximum temperature in the target is 888K for the inlet velocity of 1.1m/sec and 764K for the inlet velocity of 2.0m/sec. The maximum temperature region is the same as the first case. Figure 4 shows the temperature distribution and the velocity vector profile in the target for the inlet velocity of 1.1m/sec. As shown in Figure 4, the maximum temperature is 888K and the maximum velocity is 3.13m/sec. Compared to the first case, the maximum temperature decreases by about 400K for the inlet velocity of 1.1m/sec and about 200K for the inlet velocity of 2.0m/sec. The reason for this is that the Pb/Bi flow is more brisk than the first case because the middle region of target is narrowed. The velocity distribution result shows that the flow of the liquid Pb/Bi in the middle height region is three times faster than the inlet velocity.

When the proton beam penetrates the steel window, heat is also deposited in the window. The third case includes the steel beam window in calculation, which is shown in Figure 2(c). The maximum temperature of this case occurs in the steel beam window region. For the beam window material, 9Cr-2WVTa is chosen since advanced martensitic/ferritic steels have advantages in radiation damage and thermal properties. The thickness of the beam window is 2mm. The heat generation rates in the beam window are estimated by using LAHET. Table 3 represents the heat generation rates in each position of the beam window. The maximum temperature of the window is 1951K for the inlet velocity of 1.1m/sec and 1716K for the inlet velocity of 2.0m/sec. These temperatures are not allowable for the steel window. Figure 5 shows the temperature distribution and the velocity vector profile of the target and the window region for the inlet velocity of 2.0m/sec. As shown in Figure 5, the maximum temperature is 1716K and the maximum velocity is 5.69m/sec. Table 4 shows the calculation result of the maximum temperature for each case.

III-2. Parabolic Intensity Proton Beam

The calculations of the parabolic proton beam case were performed in the same geometry as the uniform proton beam case. In the first case, the maximum temperature of the target is 1865K for the inlet velocity of 1.1m/sec and 1303K for the inlet velocity of 2.0m/sec. These values are about 400~600K higher than those of the uniform intensity proton beam case. Figure 6 shows the temperature distribution and the velocity vector profile in the target for the inlet velocity of 2.0m/sec case. As shown in Figure 6, the maximum temperature is 1303K in the below region of the window and the maximum velocity is 3.22m/sec in the outlet region.

In the second case, the maximum temperature in the target is 1081K for the inlet velocity of 1.1m/sec and 871K for the inlet velocity of 2.0m/sec. The maximum temperature region is the same as the first case. Figure 7 shows the temperature distribution and the velocity vector profile in the target for the inlet velocity of 2.0m/sec. Compared to the first case, the maximum temperature decreases by about 800K for the inlet velocity of 1.1m/sec and about 400K for the inlet velocity of 2.0m/sec.

In the third case calculation, the maximum temperature of the window is 2550K for the inlet velocity of 1.1m/sec and 2081K for the inlet velocity of 2.0m/sec in the steel beam window region. These temperatures exceed the beam window melting temperature. Therefore,

that is not allowable for the steel window. Table 5 represents the heat generation rates in each position of the beam window. Figure 8 shows the temperature distribution and the velocity vector profile of the target and the window region for the inlet velocity of 2.0m/sec. Table 6 shows the calculation result of the maximum temperature for each case. Based on these calculations, the beam window can be damaged by high temperature and thermal stress. So, the independent cooling system for the beam window must be considered.

III-3. Double Window System

We estimated the temperature distribution for the double window system. The double window system consists of the 2mm thick inner and outer windows and the liquid Pb/Bi flows through a 4mm wide channel between inner and the outer windows as shown in Figure 9. In the double window system, it is assumed that the liquid Pb/Bi flows in one direction. In calculation of this study, we used an orthogonal coordinate transformation. The coolant flowing direction is x-directional coordinate and the vertical direction of the coolant flowing is the y-directional coordinate. Table 7 shows the computational cells in the double window calculation. The spacing of the y-directional cells is 1mm. We used the same heat generation rates for the inner and outer windows, which are shown in Table 3 and 5. The upper surface of the inner window is assumed to be adiabatic and the heat transfer of the lower surface of the outer window is treated by the heat transfer coefficient obtained by the calculation of case 3. In calculation of case 3, the heat transfer coefficients near the beam window are varied from ~13000W/m^{2}K (bottom inlet velocity : 1.1m/sec) to ~23000W/m^{2}K (bottom inlet velocity : 2.0m/sec).

In the uniform intensity proton beam case, it is revealed by the sensitivity analysis that the inlet velocity of the Pb/Bi coolant, which flows through the narrow channel, must be equal or larger than 6m/sec to maintain the maximum window temperature below 1200K by the sensitivity analysis. Therefore, the inlet velocity of the Pb/Bi coolant flowing the narrow channel is set to be 6.0m/sec in this calculation. Figure 10 shows the temperature distribution in the double window of the uniform intensity proton beam. Figure 10 is the result of that the heat transfer coefficient obtained in the 2.0m/sec bottom inlet velocity of the case 3 calculation is adopted as the outer window boundary condition. The maximum temperatures in the inner and outer windows are presented in Table 8. The maximum temperature in the inner window is barely affected by the heat transfer coefficient of the lower surface of the outer window. The maximum temperature in the outer window elevates to 925K for the 1.1m/sec bottom inlet velocity of the case 3 and to 870K for the 2.0m/sec bottom inlet velocity.

In the parabolic intensity proton beam case, the maximum temperatures in the inner and outer windows are presented in Table 9. The maximum temperature in the inner window elevates to 1870. This value is higher than the window melting temperature. So, the inlet velocity of the Pb/Bi coolant flowing the narrow channel must be larger than 6.0m/sec. The maximum temperature in the outer window elevates to 1350K for the 1.1m/sec bottom inlet velocity of the case 3 and to 1200K for the 2.0m/sec bottom inlet velocity. These results show that the temperature elevation in the window is mitigated in the double window system compared to the single window system.

IV. CONCLUSION

The CFD analytical results of the liquid Pb/Bi target have been presented in this paper. Based on the 2-D analysis, the temperature and velocity distributions are investigated. The temperature varies rapidly in the region just below the center of the beam window, and is almost uniform in the other region. When we did not include the beam window in the

calculation, the maximum temperature position is located below beam window. In the case of the narrowed target, the maximum temperature decreases by about 200~400K or 400~600K due to brisk flow of the liquid Pb/Bi. Therefore, further study for these structures is needed. In the calculation including the beam window, the maximum temperature position occurs in the steel window region. The results show that the maximum temperature is too high in case of the single window and the parabolic intensity proton beam. To overcome this problem, thermal hydraulic analysis for the double window system has been performed.

V. ACKNOWLEDGMENT

This work has been supported by the Korea Ministry of Science and Technology(MOST) and the Korea Electric Power Co.(KEPCO).

REFERENCES

1. Won-Seok Park et al., "Development of Nuclear Transmutation Technology", KAERI/RR-1702/96, 1996
2. Seok-Joong Han et al., "Selection of an Optimal Coolant Material for the Sub-Critical Transmutation System", KAERI/TR-1117/98, 1998
3. V. P. Eismont, S. G. Yavshits, V. G. Khlopin, "Physical Aspects of Neutron Generation in the Target of an Accelerator Driven System", IAEA-TECDOC-985, pp. 26-31, 1997
4. X. Cheng et al., "Thermal hydraulic Investigations on Liquid Metal Target System", Proceedings of the International Conference on Heavy Liquid Metal Coolants in Nuclear Technologies, A.21, 1998
5. G. Baur et al., "The European Spallation Source Study : Final Report", ESS-96-53-M, 1997

Table 1. Heat Generation Rate in the Liquid Pb/Bi Target of Uniform Intensity Proton Beam

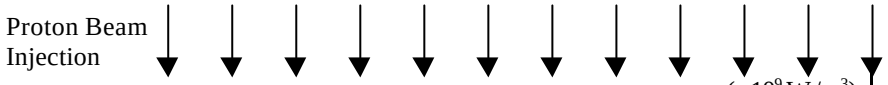

($\times 10^9$ W/m^3)

	5cm	4cm	3cm	2cm	1cm
12cm	4.94	5.39	5.27	5.31	5.06
	4.80	5.46	5.26	5.21	5.60
	4.40	4.93	5.05	5.39	5.16
	3.95	4.59	4.83	4.94	5.04
	3.66	4.33	4.45	4.46	4.84
	3.17	3.87	3.95	4.15	4.40
8cm	1.56				
15cm	0.76				
15cm	0.38				

Table 2. Heat Generation Rate in the Liquid Pb/Bi Target of Parabolic Intensity Proton Beam

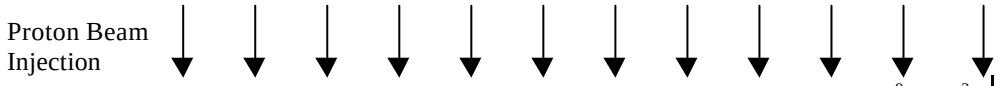

($\times 10^9$ W/m^3)

	10cm	9cm	8cm	7cm	6cm	5cm	4cm	3cm	2cm	1cm
10cm	0.02	0.03	0.06	0.12	0.26	1.94	4.86	7.14	8.73	9.64
10cm	0.05	0.07	0.12	0.19	0.42	1.39	3.01	4.30	5.23	5.68
10cm	0.05	0.07	0.10	0.19	0.39	0.92	1.63	2.26	2.71	2.98
10cm	0.04	0.06	0.10	0.18	0.31	0.55	0.82	1.08	1.29	1.36
10cm	0.04	0.06	0.09	0.14	0.22	0.32	0.42	0.50	0.60	0.64

Table 3. Heat Generation Rate in the Beam Window of Uniform Intensity Proton Beam

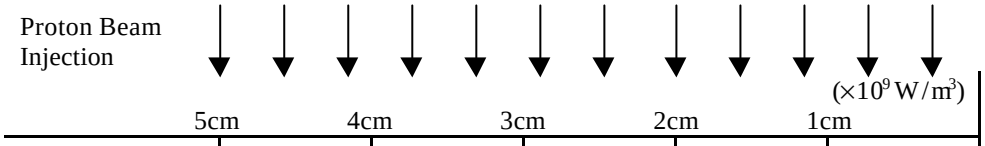

2mm	4.18	5.54	4.63	4.44	4.34

Table 4. Maximum Temperature for Each Cases of the Uniform Proton Beam

Bottom Inlet Velocity	1.1 m/sec	1.35 m/sec	1.5 m/sec	2.0 m/sec
Case-1	1287 K	1163 K	1108 K	984 K
Case-2	888 K	837 K	815 K	764 K
Case-3	1951 K	1856 K	1814 K	1716 K

Table 5. Heat Generation Rate in the Beam Window of Parabolic Intensity Proton Beam

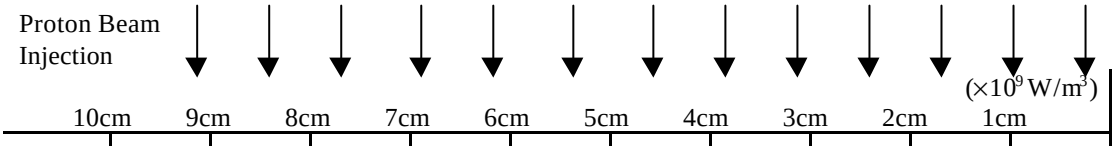

2mm	0.004	0.006	0.009	0.019	0.071	1.90	5.29	7.20	9.09	9.64

Table 6. Maximum Temperature for Each Cases of the Parabolic Proton Beam

Bottom Inlet Velocity	1.1 m/sec	1.35 m/sec	1.5 m/sec	2.0 m/sec
Case-1	1865 K	1634 K	1532 K	1303 K
Case-2	1081 K	995 K	957 K	871 K
Case-3	2550 K	2359 K	2276 K	2081 K

Table 7. Computational Cells in Double Window Calculation

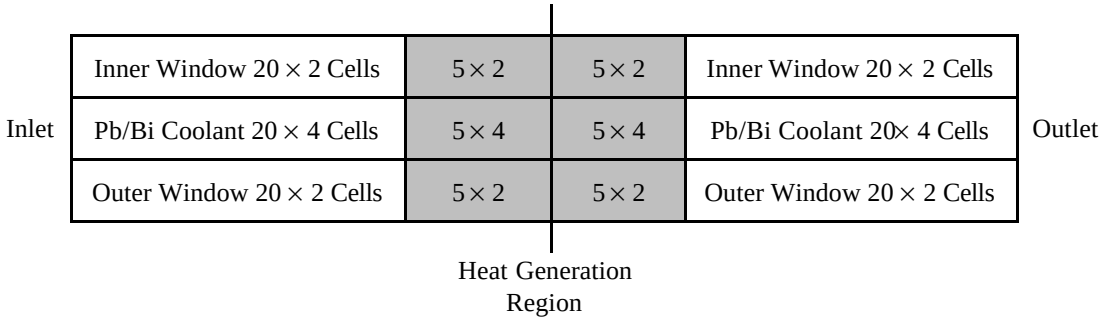

Table 8. Maximum Temperature for Double Window System of the Uniform Proton Beam

CASE-3 Bottom Inlet Velocity	1.1m/sec	1.35m/sec	1.5m/sec	2.0m/sec
Inner Window	1161K	1160K	1160K	1160K
Outer Window	925K	905K	895K	870K

Table 9. Maximum Temperature for Double Window System of the Parabolic Proton Beam

CASE-3 Bottom Inlet Velocity	1.1m/sec	1.35m/sec	1.5m/sec	2.0m/sec
Inner Window	1870K	1870K	1870K	1870K
Outer Window	1350K	1300K	1270K	1200K

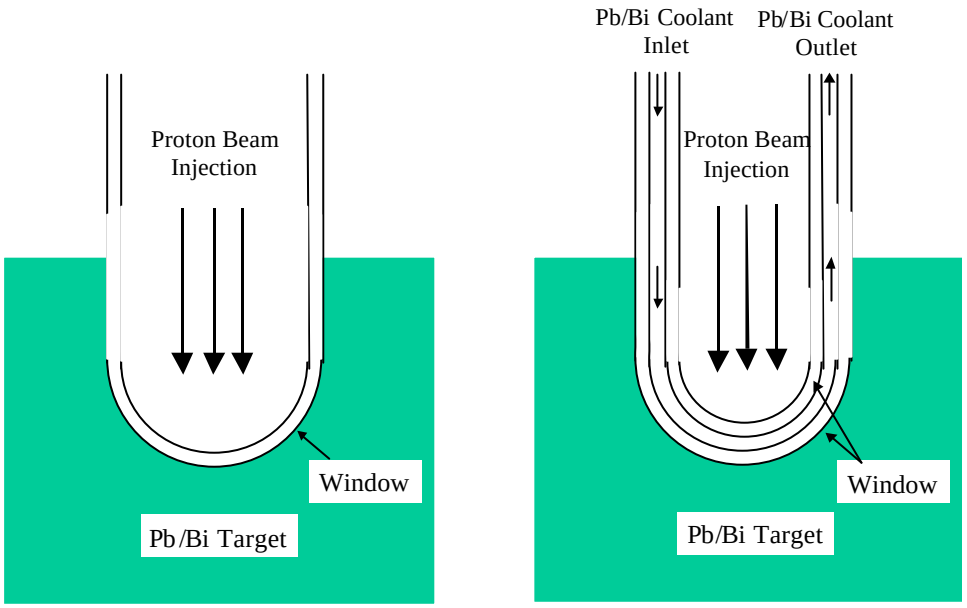

(a) Single Window System (b) Double Window System

Figure 1. Schematic Diagram of the Beam Window System

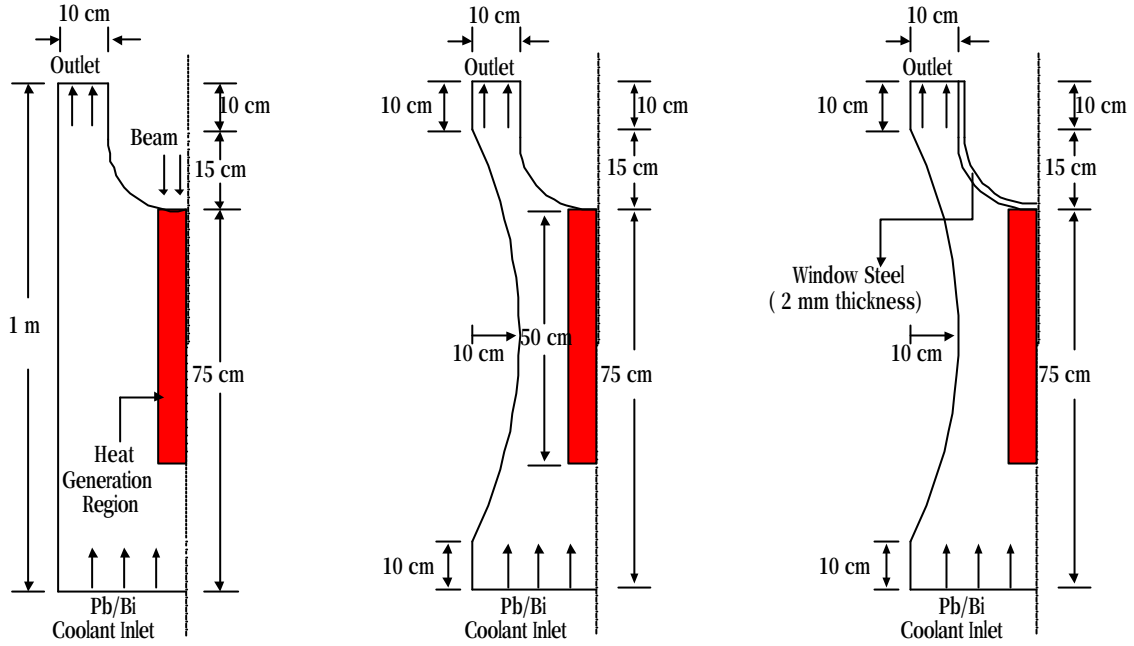

(a) Case1 (b) Case2 (c) Case3

Figure 2. Calculation Geometry of the Forced Convection Target System

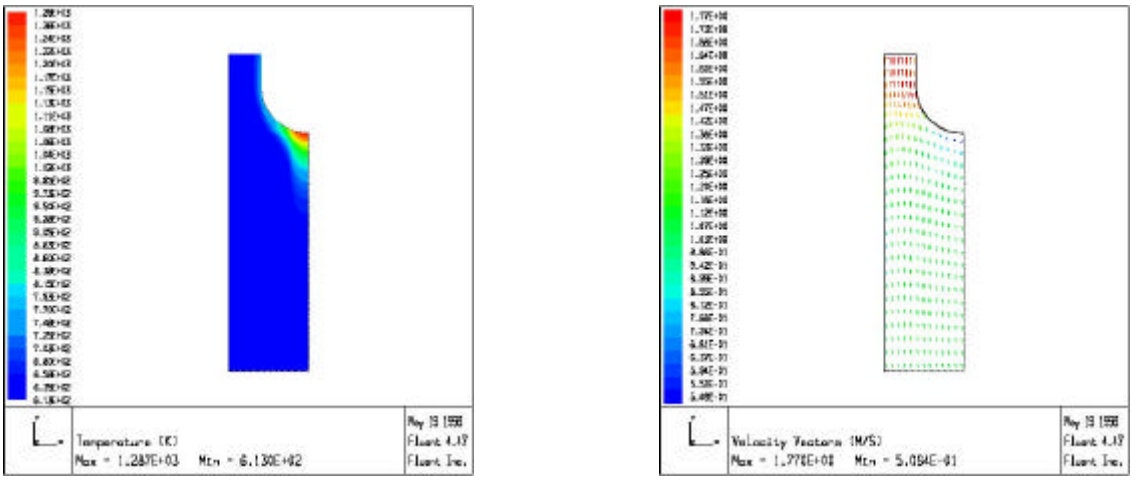

(a) Temperature Distribution (b) Velocity Vector Profile

Figure 3. Calculation Results for the Case-1 of the Uniform Proton Beam (Inlet Velocity 1.1m/sec)

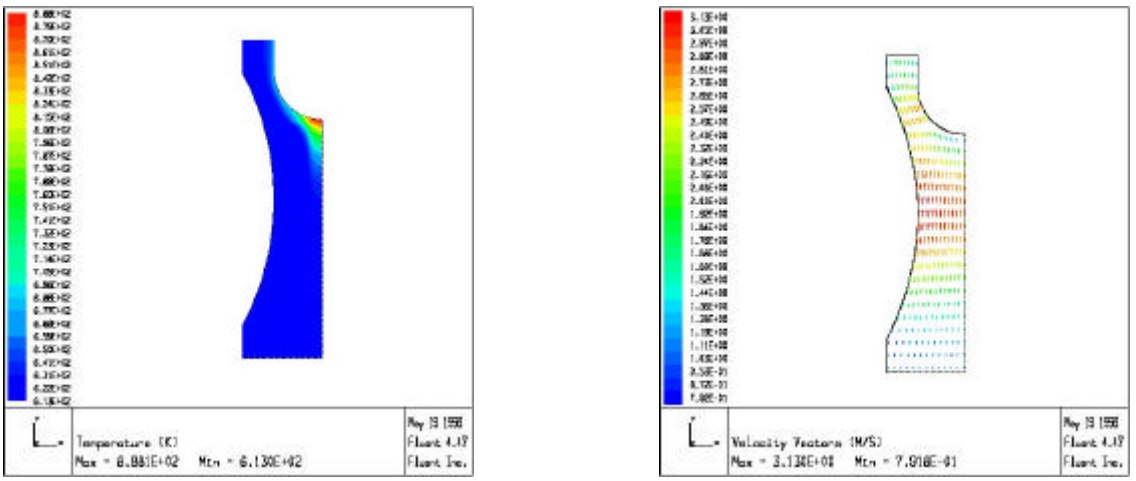

(a) Temperature Distribution (b) Velocity Vector Profile

Figure 4. Calculation Results for the Case-2 of the Uniform Proton Beam (Inlet Velocity 1.1m/sec)

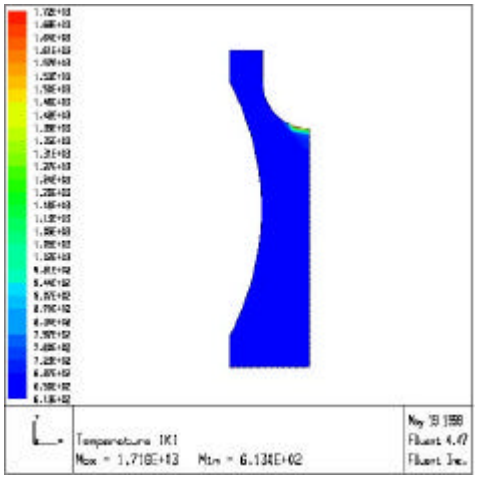

(a) Temperature Distribution

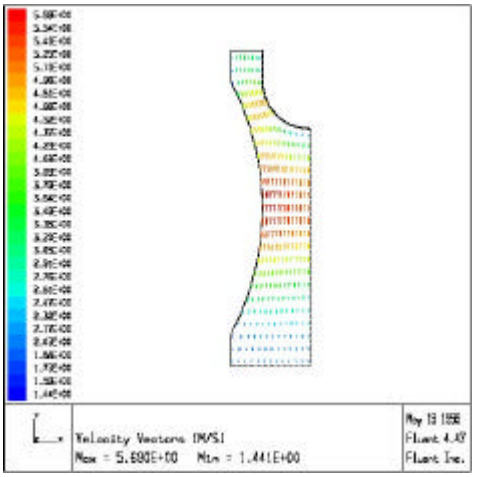

(b) Velocity Vector Profile

Figure 5. Calculation Results for the Case-3 of the Uniform Proton Beam (Inlet Velocity 2.0m/sec)

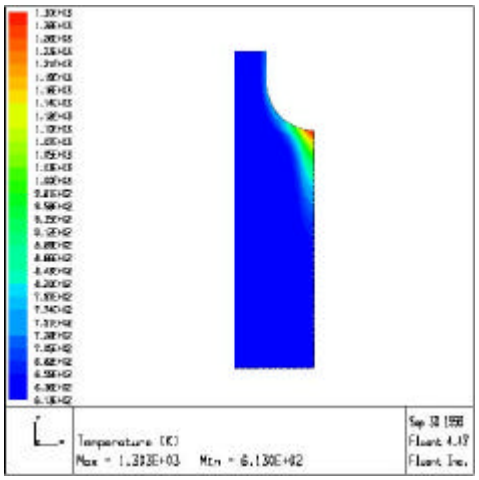

(a) Temperature Distribution

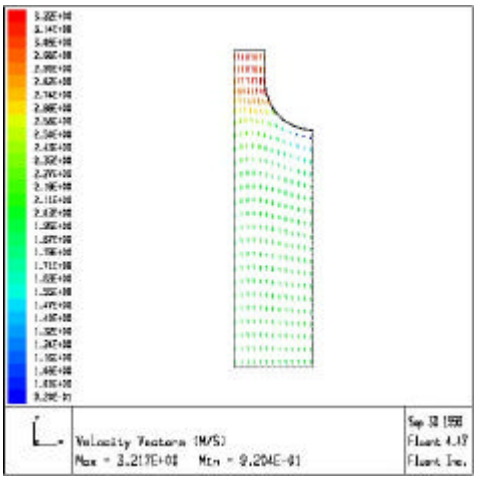

(b) Velocity Vector Profile

Figure 6. Calculation Results for the Case-1 of the Parabolic Proton Beam (Inlet Velocity 2.0m/sec)

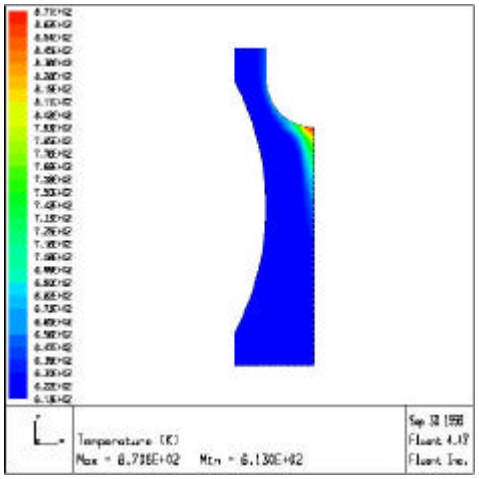

(a) Temperature Distribution

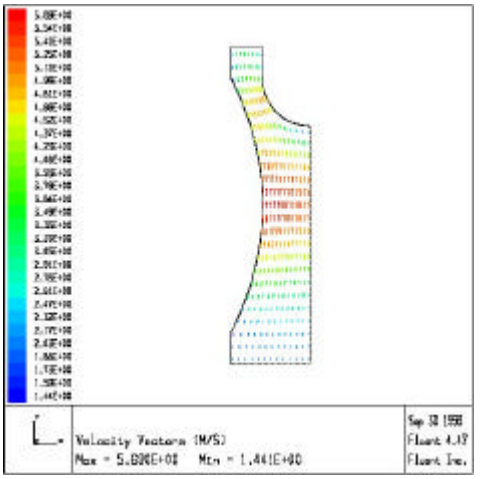

(b) Velocity Vector Profile

Figure 7. Calculation Results for the Case-2 of the Parabolic Proton Beam (Inlet Velocity 2.0m/sec)

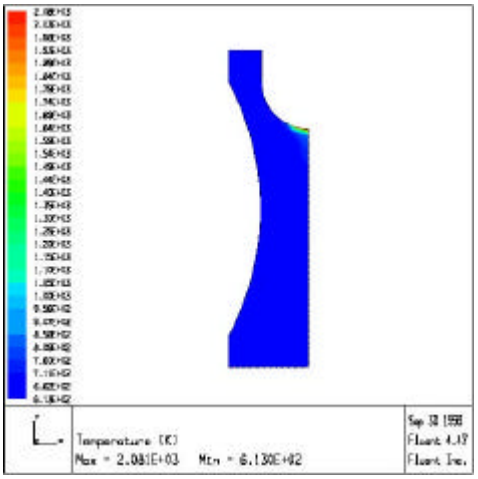

(a) Temperature Distribution

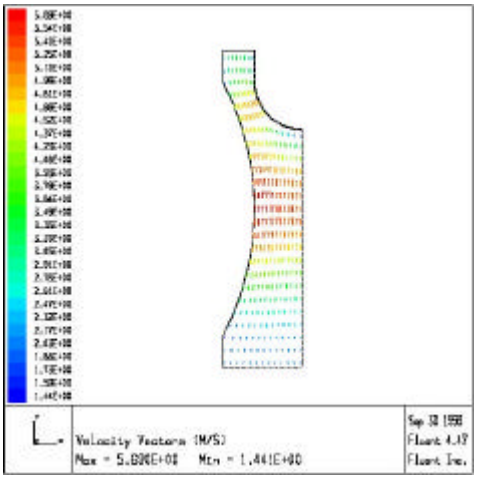

(b) Velocity Vector Profile

Figure 8. Calculation Results for the Case-3 of the Parabolic Proton Beam (Inlet Velocity 2.0m/sec)

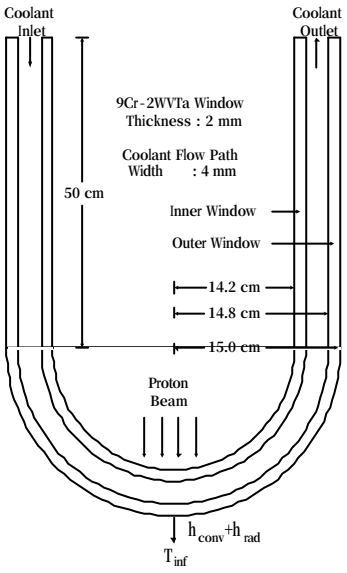

Figure 9. Double Window System

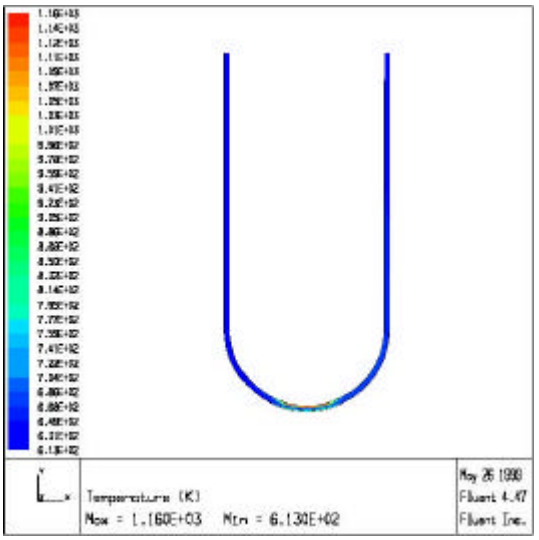

Figure 10. Temperature Distribution of Double Window